ROOM
-VENT
'90

A2

Predictions of air flow pattern in a room ventilated by an air jet. The effect of turbulence model and wall function formulation

U. Renz, U. Terhaag
Lehrstuhl für Wärmeübertragung und Klimatechnik
Aachen University of Technology
Aachen, FRG

PREDICTIONS OF AIR FLOW PATTERN IN A ROOM VENTILATED BY AN AIR JET. THE EFFECT OF TURBULENCE MODEL AND WALL FUNCTION FORMULATION

U. Renz, U. Terhaag
Lehrstuhl für Wärmeübertragung und Klimatechnik
Aachen University of Technology
Aachen, FRG

SUMMARY

Numerical predictions of room air movement were carried out for a non isothermal two-dimensional test room using the k,ε- turbulence model and an algebraic Reynolds stress model and two different wall function formulations from literature. The numerical results show that there is no remarkable difference between different wall functions as long as a minimum distance of the first grid point from the wall is observed. It was found that the computed velocity and temperature fields are independent of the grid size for a grid size of (46*39) lines with an optimized grid distribution. The numerical results are in general agreement with the measured values but the predictions of the mean air velocities and the turbulence quantities with the algebraic Reynolds stress model are closer to the experimental values as with the k,ε-turbulence model.

Introduction

Numerical calculation techniques based on the conservation equations for turbulent flows are widely used nowadays in industry to predict flow configurations. Several computer codes are commercially available. These computer codes are more and more applied by the air conditioning industry to design air ventilating systems and to simulate air flow patterns in ventilated rooms in order to replace expensive and time consuming experiments.

The application of such codes is restricted mainly by two facts. First the turbulence models incorporated are still doubtful for flow fields with low air velocities and high turbulence levels and not thoroughly approved by experimental data. Furthermore most of the practical problems to be solved need large computer storage and computer time. So-called wall functions have to be incorporated in the near wall regions to avoid excessive grid numbers and low Reynolds number corrected turbulence models in that area. The effect of these modifications on the predicted will be investigated in this paper.

Theoretical Basis

Conservation Equations

The governing conservation equations to describe velocity, temperature and humidity fields in a room are the

- continuity equation
- momentum equation
- energy equation
- vapor concentration equation

These partial differential equations can be written in a general form

$$\frac{\delta(\rho u_j \phi)}{\delta x_j} = \frac{\delta}{\delta x_j}\left(\Gamma_\phi \frac{\delta \phi}{\delta x_j}\right) + S_\phi \qquad (1)$$

The definitions of the general variables ϕ, the effective transport properties Γ_ϕ and the source terms S_ϕ are given in table 1. As can be seen from table 1 the buoyancy terms are included in the momemtum equation but there is no source term in the energy equation which means that the diffusional transport of enthalpy in the room air is partly neglected.

Turbulence Models

k,ε-Turbulence Model. Prediction of turbulence has been attempted in this paper by two models. The first one is the well known k,ε-model given by Launder and Spalding (1) which uses two additional equations, one for the kinetic energy of turbulence k and one for the dissipation of this quantity ε. These transport equations are of the same form as the conservation equations. The appropriate definitions and constants are given in table 1 and table 2 respectively.

	ϕ	Γ_ϕ	S_ϕ
continuity	1	0	0
momentum	u_i	η_{eff}	$-\frac{\delta\rho p}{\delta x_i} - \frac{2}{3}\frac{\delta}{\delta x_i}\rho k - \rho g_i$
energy	h	$\frac{\eta_{eff}}{Pr_{eff}}$	0
turb. energy	k	$\frac{\eta_{eff}}{\sigma_{k,eff}}$	$\eta_{eff}\left(\frac{\delta u_i}{\delta x_j}+\frac{\delta u_j}{\delta x_i}\right)\frac{\delta u_i}{\delta x_j} - \rho\varepsilon$
dissipation	ε	$\frac{\eta_{eff}}{\sigma_{\varepsilon,eff}}$	$\frac{\varepsilon}{k}\left(C_{1,\varepsilon}\,\eta_{eff}\left(\frac{\delta u_i}{\delta x_j}+\frac{\delta u_j}{\delta x_i}\right)\frac{\delta u_i}{\delta x_j} - C_{2,\varepsilon}\,\rho\varepsilon\right)$

Table 1. General variables ϕ, effective transport properties Γ_ϕ and source terms S_ϕ of the conservation equations.

C_η	$C_{1,\varepsilon}$	$C_{2,\varepsilon}$	σ_k	σ_ε
0.09	1.44	1.92	1.1	1.3

Table 2. Constants of the conservation equations.

Reynolds Stress Model. In swirling or recirculating flows and also in flows with low velocities and high turbulence levels which are found frequently in room air applications the k,ε-model which is based on the assumption of an isotropic turbulence structure may not be appropriate. For near equilibrium anisotropic flows the so-called algebraic Reynolds stress model was proposed.where the Reynolds stress terms are proportional to the kinetic energy of turbulence. This model is explained in detail by Launder (2).

Effective Transport Properties. The effective viscosity is evaluated from equation (2)

$$\eta_{eff} = \eta_t + \eta_l \qquad (2)$$

where η_t can be derived from

$$\eta_t = C_\eta \rho \frac{k^2}{\varepsilon}$$

(3)

using the local values of k and ε and the constant C_η from table 2.

Wall Functions

To treat the near wall region of the flow by a solution of the general conservation equations an extension to the turbulence model is needed which takes into account the damping influence of the wall. Such a low Reynolds number turbulence model was proposed by Jones and Launder (3). This model was successfully used for several problems of the boundary layer type, see i.e. (4) or (5). But the extra amount of grid lines in the neighborhood of the wall is prohibitive for elliptic flow configurations, at least for the existing computer systems.

Therefore most industrial applications make use of the so-called wall functions which serve as boundary conditions in the solution procedure. To derive these algebraic relationships a Couette-flow is assumed near the wall, allowing to integrate the momentum and the energy equation from the wall to a distance y within the boundary layer where the assumption of the Couette flow is still valid. Defining dimensionless quanities the following equations can be derived

$$\tau^+ = 1 + m^+ u^+ + p^+ y^+$$

(4)

$$q^+ = 1 + m^+ T^+$$

(5)

with

$$y^+ = \frac{\rho u_\tau y}{\eta_l} \; ; \qquad u^+ = \frac{u}{u_\tau} \; ; \qquad T^+ = \frac{\rho u_\tau (h - h_w)}{-q_w}$$

$$m^+ = \frac{m_w}{\rho u_\tau} \; ; \qquad q^+ = \frac{q}{q_w} \; ; \qquad \eta^+ = \frac{\eta_{eff}}{\eta_l} \; ; \qquad p^+ = \frac{\eta_l \frac{\delta p}{\delta x}}{\sqrt{\rho \tau_w^3}}$$

Newton's and Fourier's law for the shear stress and the heat flux term combined with the results of Prandtl's mixing length hypothesis are applied to equ. (4) and (5) and yield after some algebraic manipulation an expression for the dimensionless velocity profile

$$u^+ = 2.5 \ln (y^+) + 5.5$$

(6)

A similar expression is found for the universal temperature profile if a relation between the effective viscosity and the dimensionless distance from the wall y^+ is assumed.

$$T^+ = \sigma_t \, (u^+ + P)$$

(7)

where the integration constant is defined by

$$P = \int_0^{u^+} \left(\frac{\sigma_l}{\sigma_t} - 1 \right) du^+$$

(8)

Numerous relations for wall functions can be found in the survey given by Jayatilleke (6). In the present paper two different formulations are chosen. The first one is the formulation by Patankar and Spalding (7) which is most commonly used in commercial computer codes, for example in the codes FLUENT (8) or PHOENICS (9), the second one is a proposal recently given by Chen (10) which was developed for room air calculations.

The main characteristics of these examples are shown in the tables 3 and 4.

y^+ - region	u^+ - function	T^+ - function	Pr_{eff}	P - function
$0 < y^+ < 11.63$	y^+	$Pr_l \, u^+$	Pr_l	-
$11.63 < y^+$	$\frac{1}{0.4187} \ln(9.783 \, y^+)$	$P_{eff} \, (u^+ + P)$	Pr_t	$8.75 \left(\frac{Pr_l}{Pr_t} - 1 \right) \left(\frac{Pr_t}{Pr_l} \right)^{0.25}$

Table 3. Wall function formulations from Patankar and Spalding (7)

y^+ - region	u^+ - function	T^+ - function	Pr_{eff}	P - function
$0 < y^+ < 8$	y^+	$Pr_l \, u^+$	Pr_l	-
$8 < y^+ < 40$	$\frac{1}{0.291} \ln y^+ + 0.853$	$\frac{1}{0.338} \ln y^+ - 0.478$	-	-
$40 < y^+$	$\frac{1}{0.435} \ln y^+ + 5.05$	$Pr_{eff} \, (u^+ + P)$	Pr_t-	$8.59 \left(\frac{Pr_l}{Pr_t} - 1 \right) \left(\frac{Pr_t}{Pr_l} \right)^{0.25}$

Table 4. Wall function formulation by Chen (10).

The resulting universal velocity and temperature profiles are shown in figure 1 and figure 2 respectively.

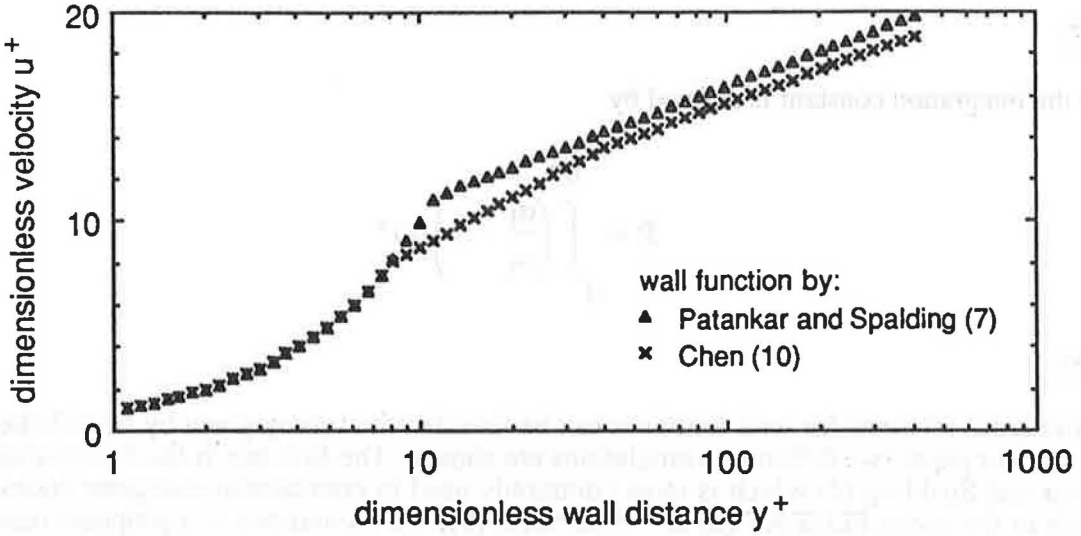

Fig. 1. Universal velocity profiles

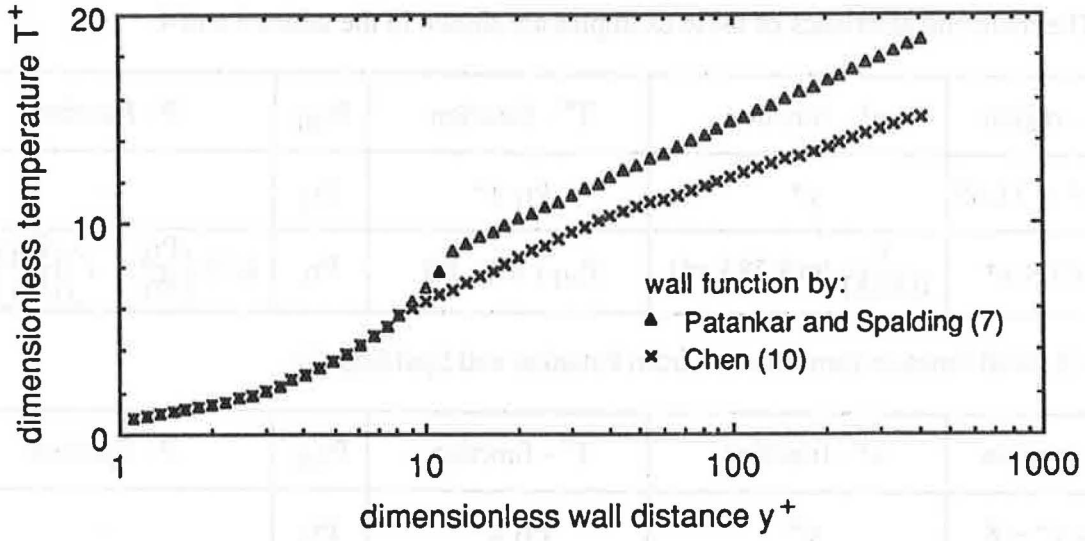

Fig.2. Universal temperature profiles

It should be mentioned that the temperature profiles are strongly dependent on the turbulent Prandtl number. Figure 2 is valid for a constant turbulent Prandtl number of $Pr_t = 0.9$.

The effect of the differences between these wall functions which were shown in figure 1 and figure 2 on the momentum or heat transfer rates and on the resulting velocity and temperature fields in the room will be discussed in the next chapter.

Solution Procedure

The system of coupled non-linear differential equations, equ.(1), which describes the conservation of mass, momentum and energy together with the boundary conditions of the problem forms the basis for the numerical calculations. They will be solved using the finite difference code FLUENT (8). Near the wall the above mentioned wall function formulations will be applied.

Some of the results of the air flow pattern in rooms will be compared with numerical results which have been presented at the Roomvent Conference 87 (11). These calculations were based on the finite difference method by Pun and Spalding (12) modified for room air calculations by Schmitz (13).

Experimental Set-up

Experimental investigations were carried out in a test room with a length of 5.9 m, a width of 3.5 m and a height of 3.6 m shown in figure 3.

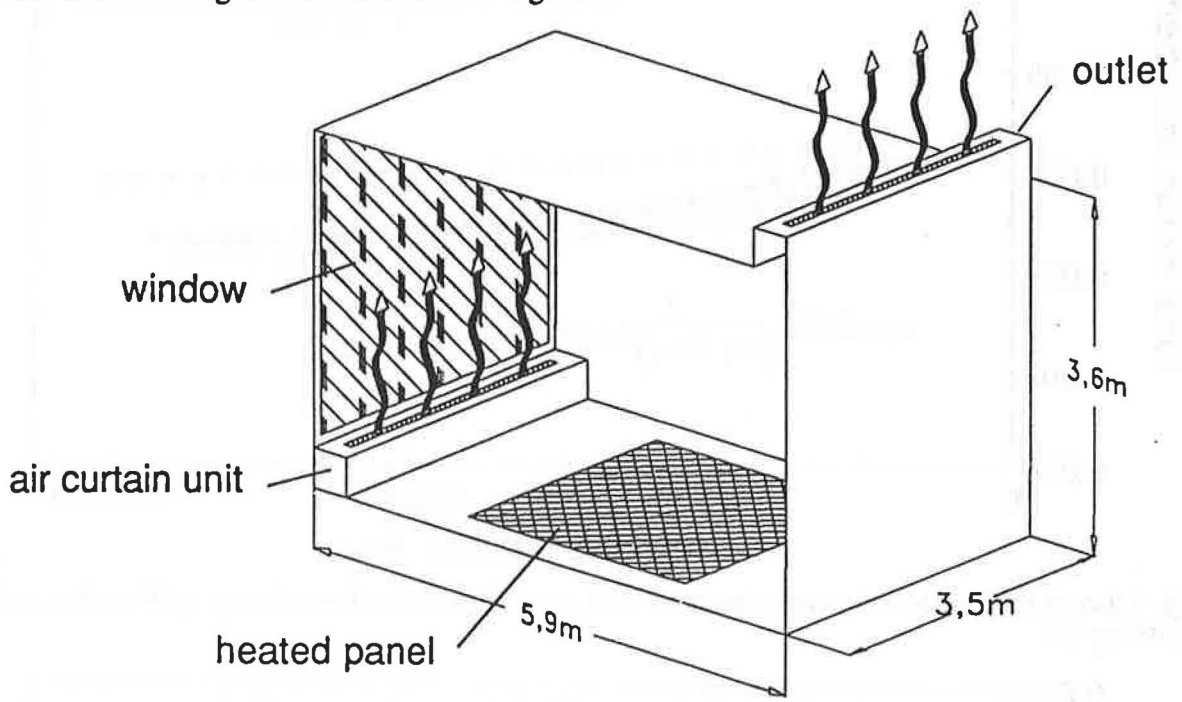

Fig.3. Experimental Set-up of the Test Room

The room air movement is established by an air curtain near a cold copper wall which simulates a window. Heat is transfered to the room by a heated floor. The heating panel could be replaced by a layer of warm water to simulate the conditions of an indoor swimming pool. All other walls are assumed to be adiabatic. Velocity measurements were carried out in the jet of the air curtain unit using a temperature compensated DISA hot wire probe, wheras the velocities within the room were measured with a TSI probe. For the temperature measurements both shielded thermocouples and Pt100 resistance thermometers were applied. It turned out that the flow is nearly two-dimensional at least for the test cases presented in this paper. For more details see (11).

Results

Friction Coefficients and Heat Transfer Coefficients for Flat Plates

Numerical prediction of the local friction coefficients and the local heat transfer coefficients on a flat plate with a turbulent boundary layer will be presented first to check the effects of the wall function formulations. A large number of tests were carried out to evaluate the number of

grid lines needed and their distribution within the boundary layer and to find out the limiting conditions for the location of the first grid point near the wall. The numerical results can be compared with known empirical formula from literature.

Local friction coefficients are shown for both the wall function formulations from Patankar and Spalding (7) in figure 4 and from Chen (10) in figure 5. As a parameter the y^+ value of the first grid point near the wall is varied.

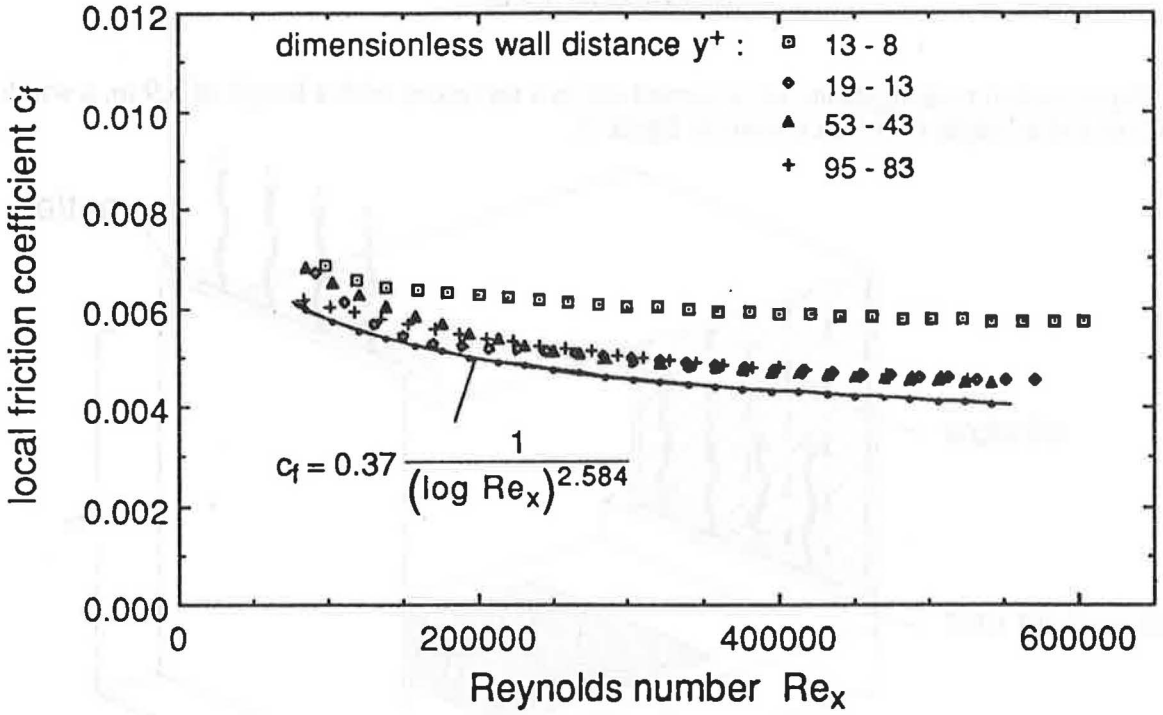

Fig. 4. Local friction coefficients calculated with the wall function formulation by Patankar and Spalding (7).

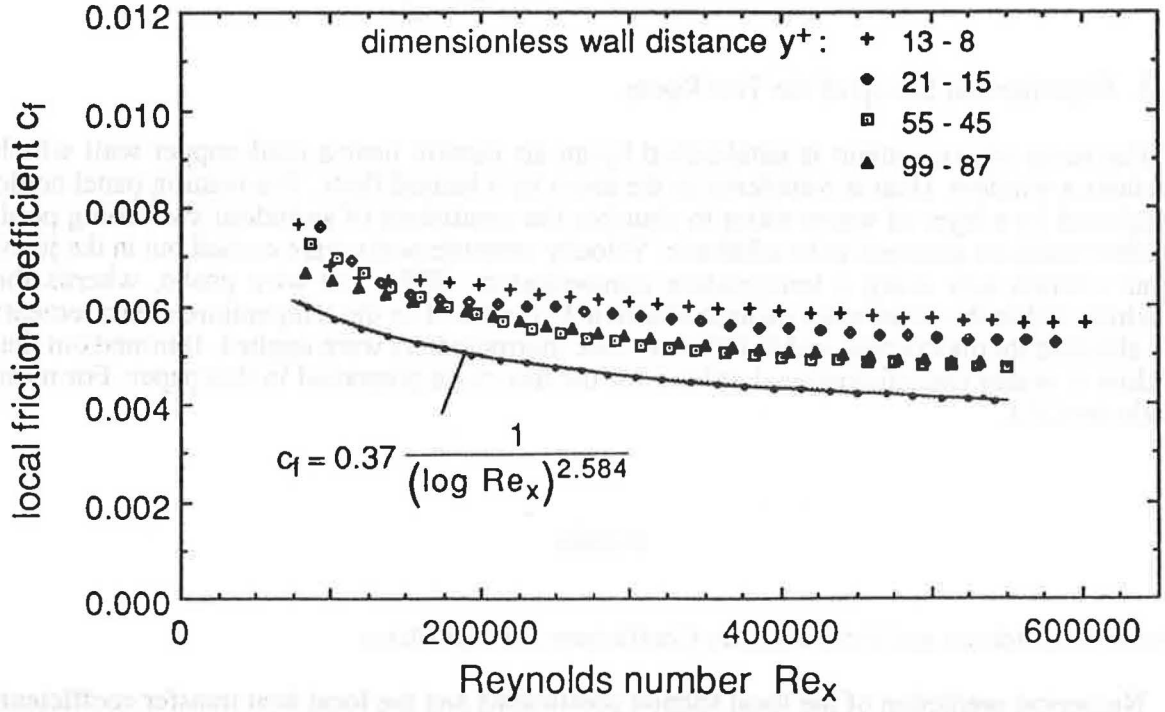

Fig. 5. Local friction coefficients calculated with the wall function formulation by Chen (10).

As can be seen from the figures both wall function formulations predict transfer coefficients which are within 10% from the empirical formula by Schulz-Grunow as long as the first grid point is located within the range $40 < y^+ < 100$. For lower values of the dimensionless distance from the wall the wall function model leads to substantial errors.

Similar results can be found for the calulated local heat transfer coefficients which are shown in figure 6 and figure 7.

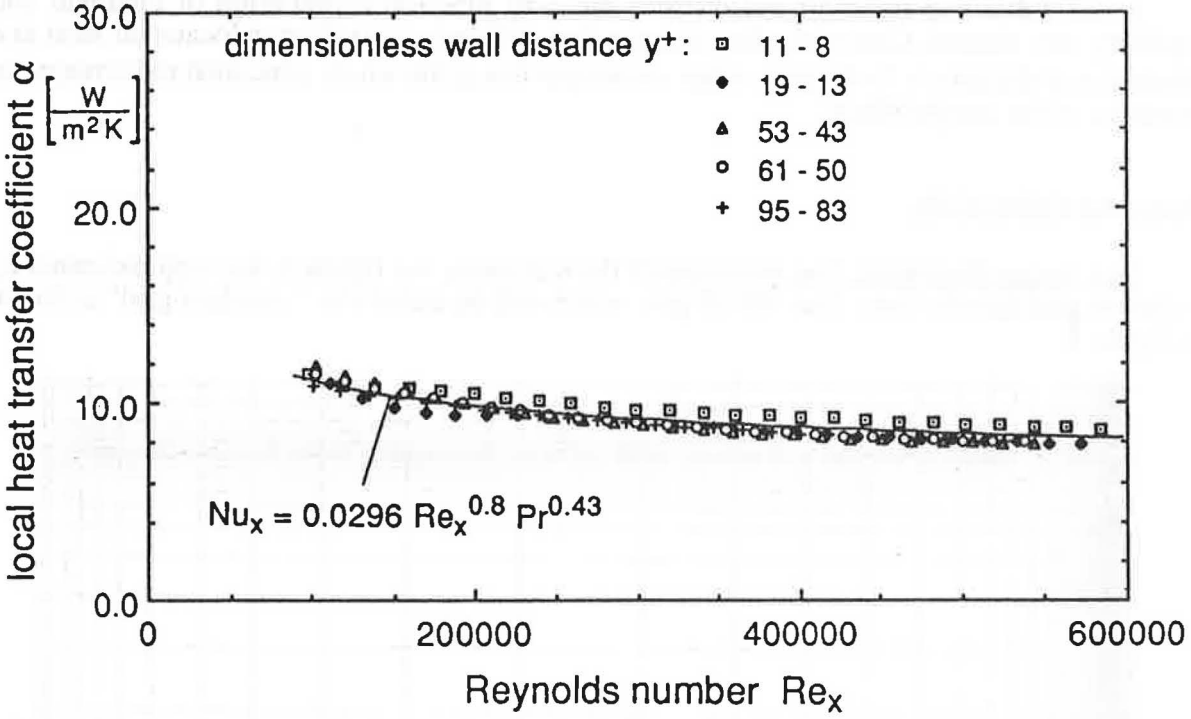

Fig 6. Local heat transfer coefficients calculated with the wall function formulation by Patankar and Spalding (7)

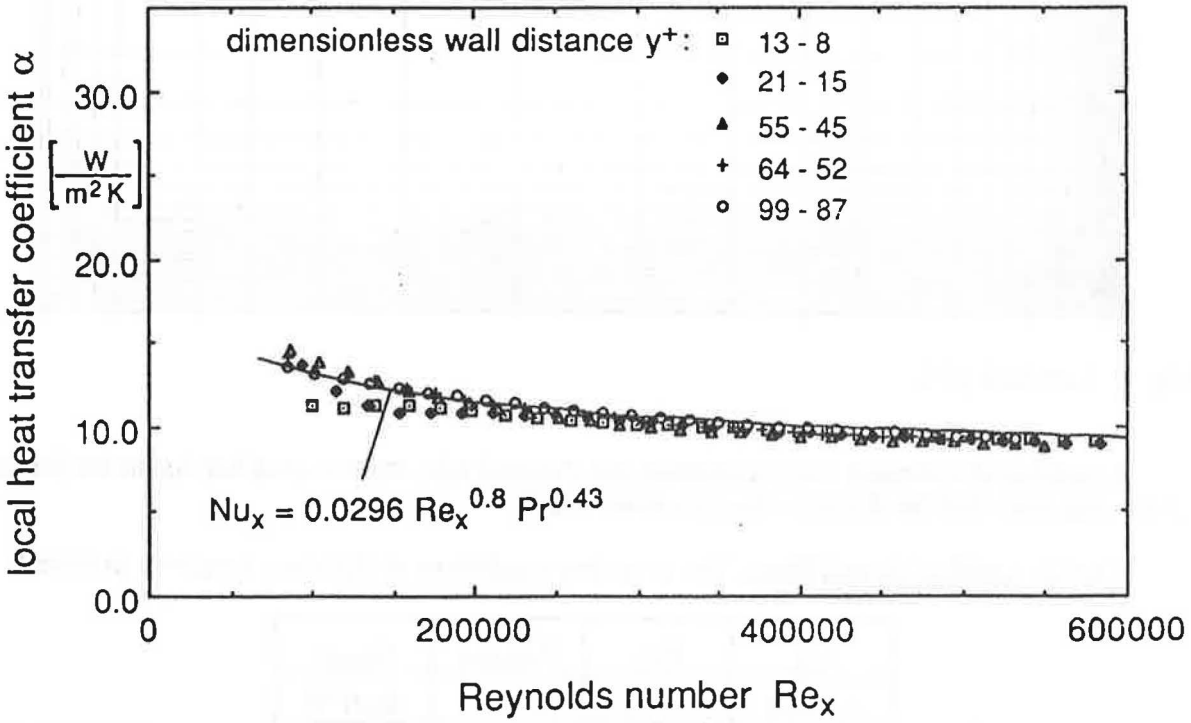

Fig 7. Local heat transfer coefficients calculated with the wall function formulation by Chen (10)

The agreement of the calculated values and the empirical correlation is again very good with both wall function formulations. The calculated values are approximately 5% lower than the results from the empirical correlation. The predictions with the Patankar and Spalding formulation is slightly more sensitive to the location of the first grid point. Similar results were found for test calculation for a turbulent pipe flow although the differences to empirical correlations for pipe flows were slightly higher.

In the following room air calculations the wall function formulation of Patankar and Spalding was chosen. Care was taken that the first grid point was always located at least at a dimensional distance $y^+ > 40$ even when extremely fine grids where generated to increase the accuracy of the computations.

Room Air Calculations

Test Room Geometry. The geometry of the test room, see figure 3, was approximated by different grid distributions. The 46*39 grid which will be called the "standard grid" is shown in figure 8.

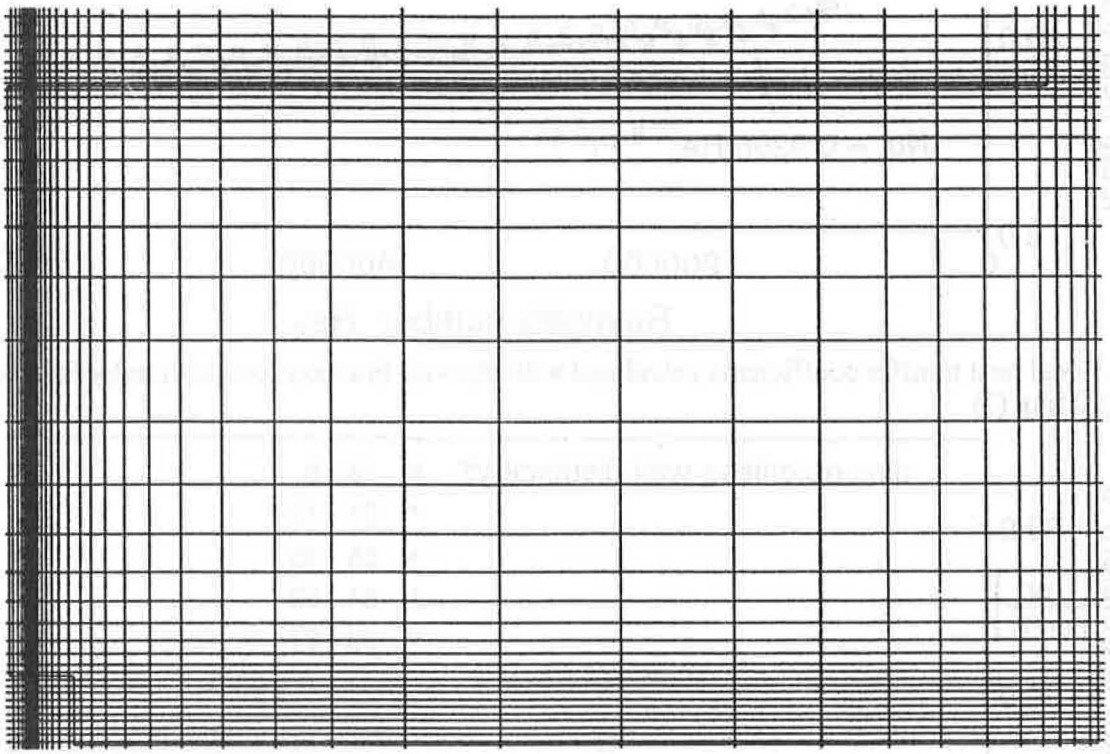

Fig. 8. Standard grid.

A number of test cases were calculated and checked with experiments but due to the limited space only one shall be discussed here in more detail.

Test Case with a Heated Floor. The boundary conditions of this case are given in table 5.

u_{ZL}	ϑ_{ZL}	ϑ_{window}	ϑ_{panel}
6.3 m/s	37.8 °C	19.3 °C	25.0 °C

Table 5. Boundary conditions for an anisothermal test situation.

The surface temperatures of the adiabatic walls were estimated by an energy balance taking into account radiative heat exchange. The resulting values are given in table 6.

$\vartheta_{ceiling}$	$\vartheta_{sidewall}$	$\vartheta_{floor\ A}$	$\vartheta_{floor\ B}$	$\vartheta_{backwall}$
26.9 °C	26.8 °C	26.6 °C	26.0 °C	26.8 °C

Table 6. Calculated temperatures of the adiabatic walls.

The predicted room air velocities and temperatures are first discussed as room mean values and compared in table 7 as well as mean fluctuation velocities and Archimedes numbers.

	exp. Ahl / Schmitz	calc. Ahl	FLUENT calc. with (7)	FLUENT calc. with (10)	FLUENT calc. with (7) and ASM
u_{RL} [m/s]	0.34	0.25	0.263	0.262	0.311
$(U^2)^{0.5}$ [m/s]	0.36	0.29	0.313	0.312	0.327
ϑ_{RL} [°C]	28.3	28.4	29.9	29.0	29.9
Ar	9580	10260	9130	10080	9080

Table 7. Comparison of experimental and predicted room mean values.

The mean values of velocity and temperature were evaluated either from the measurements (grid 17*20) at distinct locations within the room or from the computed results which were interpolated at the measuring locations. For better comparison of the characteristics of the room air flow the values within the wall jet were not taken into account.

It can be seen from the table that the choice of the wall function formulation has no influence on the results. The calculated results based on the FLUENT code with the wall functions by Patankar and Spalding (7) and Chen (10) and the calculated results by the "home made" code by Schmitz (13) which is based originally on the CHAMPION code and which also uses the wall function formulation by Patankar and Spalding give more or less the same results. All predicted mean velocity and turbulence values are roughly 25% lower and all mean temperature values are roughly 5 % higher compared to the experimental results. Only the algebraic Reynolds stress model (ASM) which takes the anisotropy of the turbulence into account shows a better agreement of the velocity values with experiments leaving the predicted mean temperatures unchanged. A further refining of the grid showed a substantial improvement of the velocity distribution within the jet nearby the window but had no remarkable effect on the room mean values which excluded this flow region. An extension of the k,ε-model to include buoyancy effects as an additional production term did not improve the situation either.

The remaining discrepancies are certainly partly due to experimental errors, too. It is well known that hot film anemometers measure too high velocity values in flows with high turbulence levels as it is the case in the core of the room air flow.

Last not least it should be remembered that the calculations are based on the assumption of a two-dimensional geometry which is not exactly the case in the present situation.

The velocity fields of the test case are shown in figure 9 to figure 12.

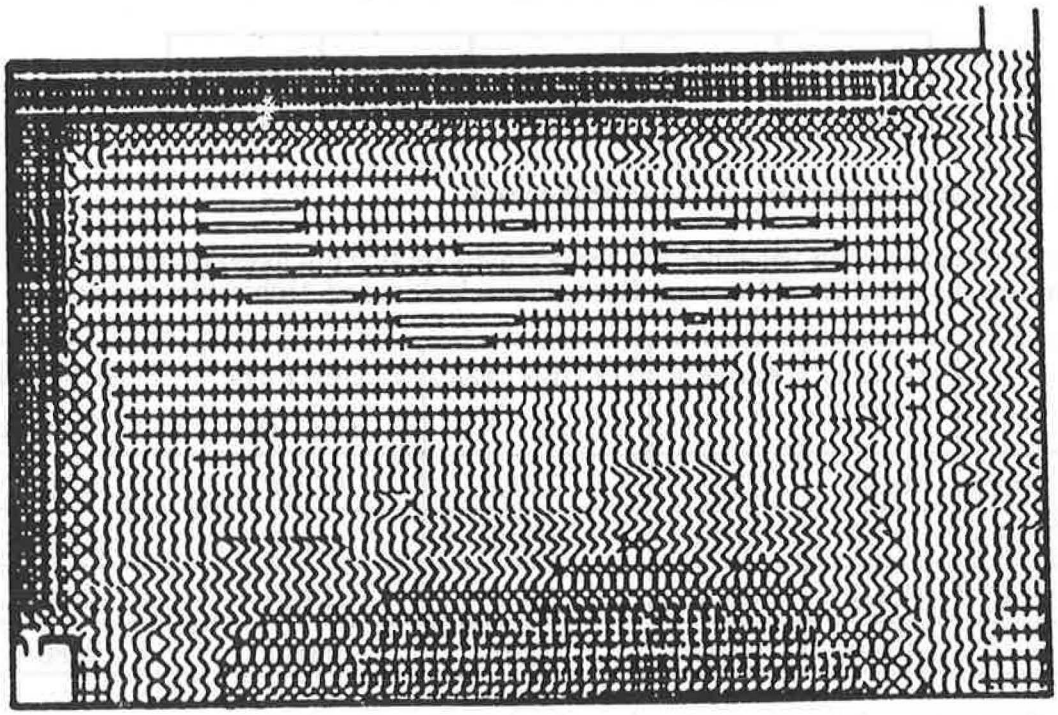

velocity symbols [m/s]:
- < 0.10 < = < 0.18 < + < 0.26 < (< 0.34 < > < 0.42
0.42 < x < 0.50 < * < 0.58 < # < 0.66 < $

Figure 9. Measured velocity field by Ahl (14)

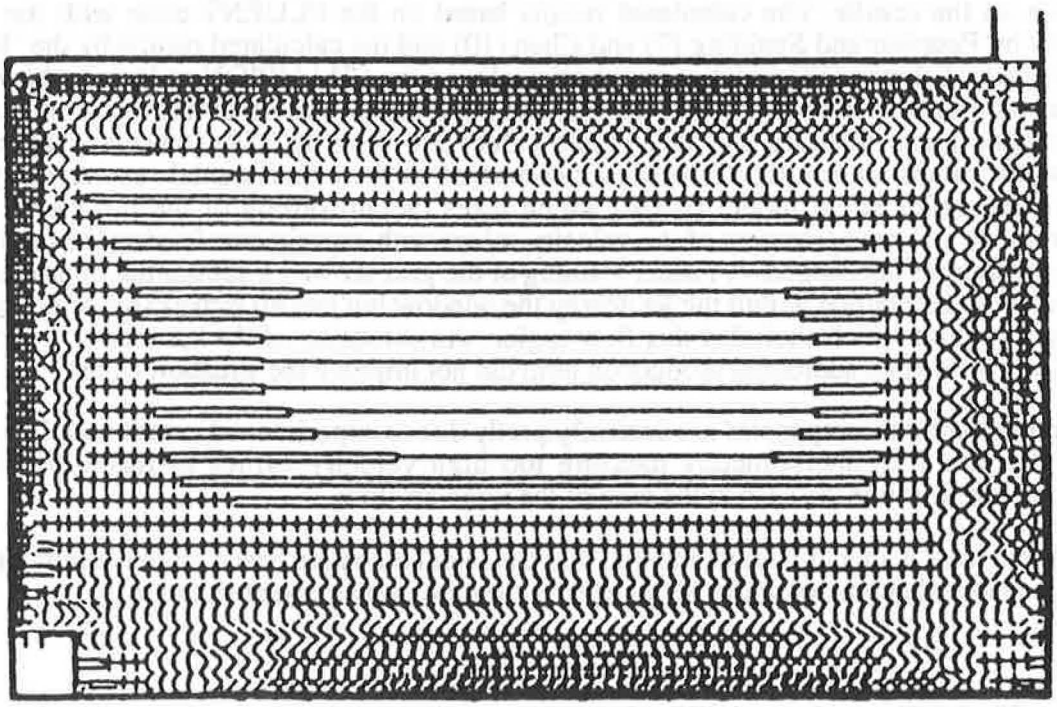

Figure 10. Calculated velocity field by Ahl (14) using the wall function formulation by Patankar and Spalding (7)and a (46 * 39) grid

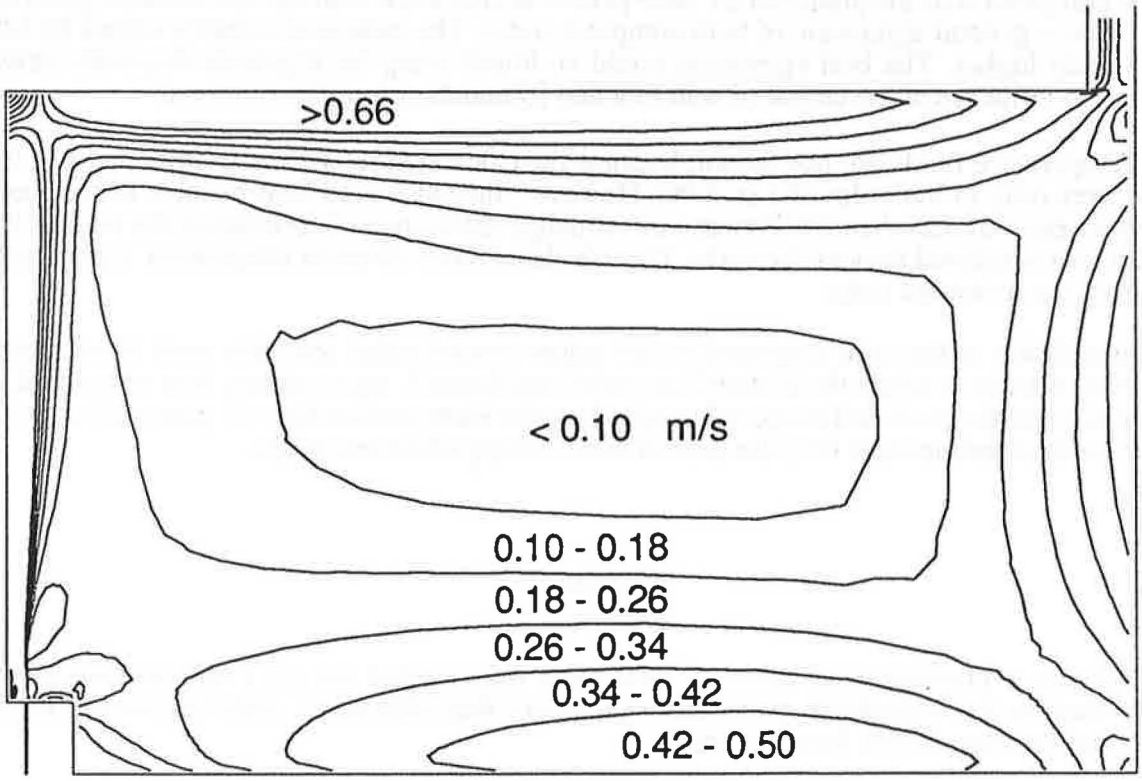

Figure 11. Calculated velocity field with FLUENT code using the wall function formulation by Patankar and Spalding (7)

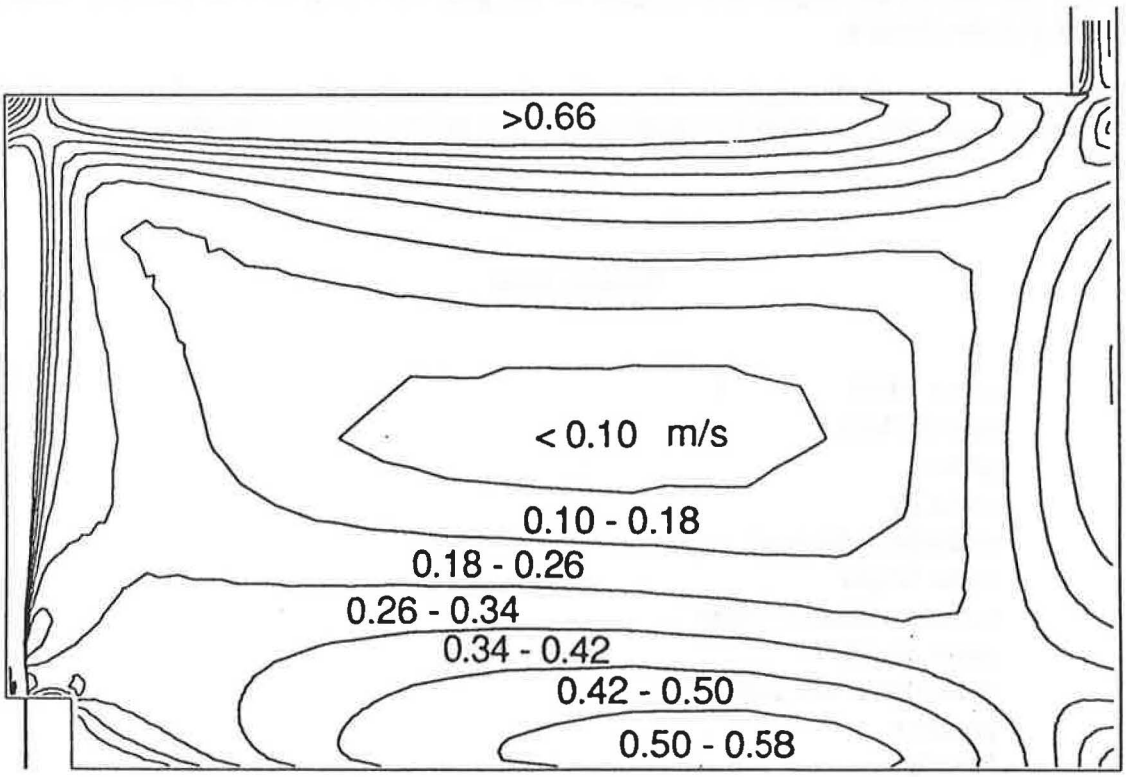

Figure 12. Calculated velocity field with FLUENT code using the wall function formulation by Patankar and Spalding (7) and the algebraic Reynolds stress model.

A comparison of the predicted air flow pattern of this work with the calculations given by Ahl shows a general agreement of both computer codes. The measured velocity values by Ahl are slightly higher. The best agreement could be found using the algebraic Reynolds stress model. No influence of the choice of wall function formulation could be observed.

Temperature fields are not shown, because the calculated temperature differences in the room were only in the order of 1 to 2 °C. However, the calculated heat balance of the room shows an error of less than 2% between the enthalpy difference inlet/outlet of the air and the overall heat transfered through the walls. The calculated room air outlet temperature agrees quite well with the measured value.

In addition to the case displayed in this paper several other test case were investigated including situations where the heated floor panel, see figure 3, was replaced by a water pool. It turned out that the predicted evaporation rate from the water surface agreed quite well with the value found experimentally from the overall mass balance of the test room.

Conclusion

Numerical predictions of room air movement were carried out for a non isothermal test room using the k,ε- turbulence model and an algebraic Reynolds stress model and two different wall function formulations from literature.

A comparison of the numerical results with experimental values shows that there is no remarkable difference between the proposed wall functions as long as the minimal dimensionless distance of the first grid point from the wall is not less than $y^+ = 40$. It was found that the results are nearly independent of the grid for a grid size of (46*39) with an optimized grid distribution.

The predictions with the algebraic Reynolds stress model are in better agreement with the experiments as with the k,ε-model because anisotropic effects of the turbulence are taken into account.

Nomenclature

B	room width
c_p	specific heat
g	gravity
h	enthalpy
h_w	enthalpy at the wall
H	room height
k	turbulent kinetic energy
L	room length
m_w	mass flux at the wall
p	pressure
q	heat flux
q_w	heat flux at the wall
u_j	velocity component
$u_o = \dot{V}/(B\,L)$	displacement velocity

u_{RL}	air mean velocity
u_{ZL}	air inlet velocity
$(\overline{U^2})^{0,5}$	fluctuation velocity
$\dot{V}$	volume flow
S_ϕ	general source term
x_j	coordinates
α	heat transfer coefficient
ϑ	temperature
ϑ_{RL}	air mean temperature
ϑ_{ZL}	air inlet temperature
ε	dissipation of turbulent kinetic energy
η_{eff}	effective viscosity
η_l	laminar viscosity
η_t	turbulent viscosity
ϕ	general variable
Γ_{eff}	effective transport property
ρ	density
ρ_{AB}	air density at outlet
ρ_{ZL}	air density at inlet
τ	shear stress
τ_w	shear stress at the wall

Dimensionless Numbers

Ar	$= \frac{2gH(\rho_{AB} - \rho_{ZL})}{u_o^2(\rho_{AB} + \rho_{ZL})}$	Archimedes number
c_f	$= \frac{\tau_w}{\rho u^2/2}$	Friction coefficient
Nu	$= \frac{\alpha x}{\lambda}$	Nusselt number
Pr	$= \frac{\eta}{\lambda / c_p}$	Prandtl number
Pr_{eff}	$= \frac{\eta_{eff}}{\lambda_{eff}/c_p}$	effective Prandtl number
Re	$= \frac{\rho u x}{\eta}$	Reynolds number
σ		general Prandtl number

References

(1) Launder, B.E. and Spalding, D.B. The numerical computation of turbulent flows. Comp. Meth. in Appl. Mech. and Engng., 1974, 3, 269-289

(2) Launder, B.E. Stress-transport closures: Into the third generation. In Proceedings of the First Symposium on Turbulent Shear Flow, Springer-Verlag, New York, 1979

(3) Jones, W.P. and Launder, B.E. The prediction of laminarization with a 2-equation model of turbulence. Intern. J.Heat and Mass Transfer, 1972, 15, 301-314

(4) Jones, W.P. and Renz, U. Condensation from a turbulent stream onto a vertical surface. Intern. J.Heat Mass Transfer, 1974, 17, 1019-1028

(5) Renz, U. and Vollmert, H. Der Wärme- und Stoffaustausch im Übergangsgebiet laminar/turbulent. Ein Vergleich von Rechnung und Experiment. Intern J. Heat Mass Transfer, 1975, 18, 1009-1014

(6) Jayatilleke, C.L.V. The influence of Prandtl number and surface roughness on the resistance of the laminar sub-layer to momentum and heat transfer. Progress in Heat and Mass Transfer, Pergamon Press, 1969, 1, 193-329

(7) Patankar, S.V. and Spalding, D.B. Heat and mass transfer in boundary layers. Intertext Books, London, 2. Ed., 1970

(8) CREARE Inc., Hanover, N.H., USA, FLUENT User Manual, Version 2.9 Update, TN-369 Rev. 3, 1+2

(9) CHAM Ltd., Wimbledon, SW 19 5AU, England, PHOENICS, Computational Fluid Dynamics

(10) Chen, O. Indoor airflow, air quality and energy consumption of buildings, Dissertation, Delft, 1988

(11) Ahl, J.P. and Renz, U. Room air movement in indoor swimming-pools. Comparison of measurements with numerical prediction. Intern. Conf. Air Distribution in Ventilated Spaces. Roomvent-87, Session 3, Stockholm, 10.-12. Juni 1987

(12) Pun, W.M. and Spalding, D.B. A general computer program for two-dimensional elliptic flows. Comp. Meth. in Appl. Mech. and Engng., 1974, 3, 269-289

(13) Schmitz, R.M. Berechnung turbulenter Raumluftströmungen bei gekoppeltem Impuls-, Wärme- und Stoffaustausch, Dissertation, RWTH Aachen, 1985

(14) Ahl, J.P. Untersuchung der Raumluftströmung bei Belüftung durch Fensterblasanlagen, Dissertation, RWTH Aachen, 1987